Electrochimica Acta 56 (2011) 4344–4350

Contents lists available at ScienceDirect

Electrochimica Acta

journal homepage: www.elsevier.com/locate/electacta

Phase identification in electrodeposited Ag–Cd alloys by anodic linear sweep voltammetry and X-ray diffraction techniques

Ts. Dobrovolska[a,*,1], I. Krastev[a], B.M. Jović[b,1], V.D. Jović[b,1], G. Beck[c], U. Lačnjevac[b], A. Zielonka[c]

[a] Institute of Physical Chemistry, Bulgarian Academy of Science, 1113 Sofia, Bulgaria
[b] Institute for Multidisciplinary Research, 11030 Belgrade, P.O. Box 33, Serbia
[c] Forschungsinstitut für Edelmetalle und Metallchemie, 73525 Schwäbisch Gmünd, Germany

ARTICLE INFO

Article history:
Received 13 October 2010
Received in revised form 15 January 2011
Accepted 17 January 2011
Available online 21 January 2011

Keywords:
ALSV
Electrodeposition
Self-organization
Silver–cadmium alloys
XRD techniques

ABSTRACT

During electrodeposition of Ag–Cd alloy coatings phenomena of self-organization and formation of spatio-temporal structures can be observed. The difficulties in the determination of the local phase composition in the observed structures are mostly connected with the strong heterogeneity of the coatings consisting of several alloy phases. The results obtained with electrochemical techniques, such as anodic linear sweep voltammetry (ALSV) are compared with results obtained by X-ray analysis and SEM. In the proposed electrolyte for dissolution of Ag–Cd alloy coatings (12 M LiCl + 0.1 M HCl) the dissolution peaks of the pure metals, Ag and Cd, have a potential difference of about 700 mV. The peaks, corresponding to the alloy phases, are situated between the dissolution potentials of Ag and Cd, their height depending on the deposition current density, i.e. on the percentage content of the alloy. Different phases (Ag, Ag_3Cd, AgCd, $AgCd_3$ and pure Cd) are observed in the coatings deposited at different cathodic potentials. A good correlation between the XRD spectra of the Ag–Cd alloy coatings and the ALSV data obtained during their dissolution is established.

1. Introduction

Alloying of silver with other metals is stimulated by the main idea to improve its tarnish resistance [1,2]. Cadmium and indium could be appropriate alloy metals to silver, because they do not tarnish and are light coloured. In fact, the alloying of silver with indium does not lead to an increase of its tarnish resistance but pattern formation has been observed on the surface of electrodeposited Ag–In alloys [3]. Later, the formation of structures, which are typical results of reaction–diffusion mechanism have been observed and studied during electrodeposition of silver with antimony [4,5], bismuth [6], tin [7] and indium [8,9]. Recently, the formation of spatio-temporal structures have been discovered also in electrodeposited silver–cadmium coatings [10].

Self-organization phenomena are observed everywhere in Nature – in the atmosphere, in geological structures, in sand dunes, during propagation of fire, in the stripes onto the body of zebras and panthers, in the spirals formed in the processes of heterogeneous catalysis etc. [11–15]. The investigation of similar processes with electrochemical methods, which are exact, due to the well defined and controlled experimental conditions, could be very effective for their understanding.

The experience gathered during electrodeposition of some silver alloys shows that the appearance of self-organization phenomena is closely connected with the phase heterogeneity of the obtained coatings [5–8].

Silver–cadmium alloys have not achieved any practical importance, but they are of considerable scientific interest, mainly because of the numerous phases formed and observed in this system [16–22]. The phase composition of these alloys could be analyzed by anodic linear sweep voltammetry (ALSV), which is an appropriate electrochemical technique for fast and precise phase analysis of thin alloy films deposited on the inert substrates [23–27].

The phases observed in the silver–cadmium alloy system are described in the monograph of Hansen and Anderko [28] in the following way:

The solubility of Cd in Ag (**α-**phase) reaches 42 at.%. In the composition range between 26 and 29 at.% Cd the high-temperature Ag_3Cd phase could be observed [29].

In the composition range between 42 and 60 at.% Cd, three phases (β, β′ and ζ) are established in the vicinity of 50 at.% Cd at different temperatures. The β- and β′-phases are characterized by the b.c.c. lattices, and the ζ-phase by h.c.p. lattice. These phases correspond to the AgCd compound. The existence of several phases (γ, γ′, ε and η) is reported in the composition range between 60

* Corresponding author. Tel.: +359 2 979 2595; fax: +359 2 873 49 68.
E-mail address: tsvetina@ipc.bas.bg (Ts. Dobrovolska).
[1] ISE member.

0013-4686/$ – see front matter © 2011 Elsevier Ltd. All rights reserved.
doi:10.1016/j.electacta.2011.01.028

and 100 at.% Cd. The first one (γ) is a hexagonal phase and the second one (γ′) possesses a b.c.c. lattice. They correspond to the Ag_5Cd_8 compound. The pure hexagonal ε-phase exists in the range 68–81.4 at.% Cd and corresponds to the Cd_3Ag compound. In the composition range 81.4–96.9 at.% Cd ε-phase exists together with the η-phase, which is a solid solution of Ag in Cd. Pure η-phase is observed in the interval 96.9–100 at.% Cd (100 °C).

In the present paper an attempt was made to determine the phase composition of silver–cadmium coatings (deposited at different conditions) by ALSV technique and to compare the results with those, obtained by XRD and SEM techniques.

2. Experimental

The cadmium, silver and the alloy coatings were deposited from cyanide electrolytes. Pure Cd from the solution containing 0.14 M $CdSO_4 \cdot 8/3\ H_2O$ + 0.56 M KCN, pure Ag from the solution containing 0.032 M $KAg(CN)_2$ + 0.56 M KCN and Ag–Cd alloys from the solution containing 0.032 M $KAg(CN)_2$ + 0.14 M $CdSO_4 \cdot 8/3\ H_2O$ + 0.56 M KCN. Chemical substances of *pro analisi* purity and distilled water were used. The experiments were performed in a 100 cm^3 tri-electrode glass cell at room temperature. The vertical working electrode (area 3 cm^2), and the two counter electrodes were made from platinum. An Ag/AgCl reference electrode was used. The reference electrode was placed in a separate compartment filled with 3 M KCl solution. It was connected to the electrolyte cell by a Haber–Luggin capillary through an electrolyte bridge containing also 3 M KCl solution.

The experiments were carried out at room temperature by means of a computerized potentiostat/galvanostat Reference 600 (Gamry Instruments Inc.) using the software PHE 200, or PAR 263 A potentiostat/galvanostat using the software Soft Corr II.

The alloy coatings were deposited under potentiostatic, or galvanostatic conditions at room temperature.

In order to determine the current efficiency for the deposition of each metal, as well as their dissolution potentials, Ag and Cd were deposited from cyanide electrolytes at different potentials (−1.0, −1.4, −1.6, −1.8 and −2.0 V) with a constant electrical charge of $Q = 1.3\ C\ cm^{-2}$ using "potential controlled coulometry" technique and then dissolved in the chloride electrolyte described below. The thickness of the films, obtained at the potentiostatic and galvanostatic conditions is between 0.7 and 1 μm. The ALSV experiments were carried out immediately after XRD investigations, the later performed immediately after the deposition of each alloy sample. The cadmium, silver and alloy coatings were dissolved in the tri-electrode cell for ALSV experiments with platinum counter electrode and Ag/AgCl reference electrode in a solution containing 12 M LiCl + 0.1 M HCl.

All potentials are given vs. Ag/AgCl electrode.

The cadmium or silver distribution on the surface of the coatings was examined by EDX-technique.

X-ray diffraction patterns for phase identification of the alloy coatings deposited at a constant potential were recorded in the angle interval 20–110° (2θ), on a Philips PW 1050 diffractometer, equipped with Cu-Kα tube and scintillation detector.

The phase composition of the alloy coating deposited at a constant current density was investigated by X-ray analysis in the 2θ range of 20°–85° with the D8 Discover diffractometer (Bruker axs) in the Bragg-Brentano diffraction geometry. The measurements were performed with Cu-Kα radiation.

For qualitative phase analysis the Eva routine (Bruker axs) on the basis of the powder diffraction file (PDF 2, Version Sep. 2004) was used.

The surface morphology of the coatings was studied by optical microscopy and scanning electron microscopy (SEM).

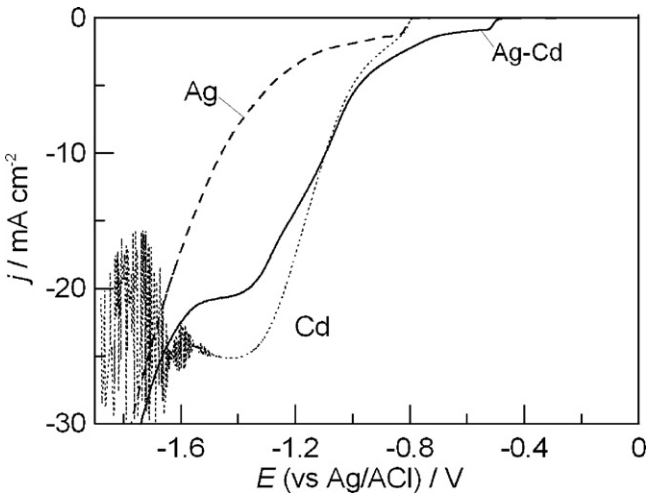

Fig. 1. Polarization curves recorded at the sweep rate of 1 mV s^{-1} for deposition of pure Ag (dashed line), pure Cd (dotted line) and Ag–Cd alloy (solid line).

3. Results and discussion

3.1. Polarization curves for Ag, Cd and Ag–Cd electrodeposition

Fig. 1 shows polarization curves obtained with a sweep rate of 1 mV s^{-1} in the electrolyte containing both metals separately or together. The initial potential of the voltammetric scan is 0 mV. The deposition of Ag (dashed line) is characterized by the cathodic shoulder, which is most likely indication of the diffusion limiting current density (taking into account small concentration of Ag) at a potential of about −0.82 V, with the deposition starting at about–0.79 V. The increase of the current at potentials < −1.2 V during the Ag deposition is connected with the reaction of hydrogen evolution. The dotted line curve in Fig. 1 corresponds to cadmium electrodeposition. The process of deposition commences at about −0.79 V and at potentials more negative than −1.6 V current oscillations with amplitude higher than 200 mV have been observed in both scan directions. Probably, the oscillations start at a potential determined by the onset of the massive hydrogen evolution during the cadmium deposition.

The phenomenon of potential oscillations under galvanostatic conditions during electrocrystallization of cadmium from alkaline cyanide solutions has been observed and reported by Kaneko et al. [30]. There are not any known reports about current oscillations in this system under potentiostatic conditions.

In the case of Ag–Cd alloy deposition a shoulder representing diffusion-controlled deposition of Ag (solid line) appears at about −0.51 V (for about 0.3 V more positive than the shoulder of pure Ag deposition). At the same time deposition starts at about −0.48 V. Hence, in the solution containing both metal ions Ag starts to deposit at more positive potential. In order to find out the reason for such behavior the analysis of Ag complexes with cyanide has been performed. The results are presented in Table 1. As can be seen, when pure Ag is present in the KCN solution the dominant complex is $[Ag(CN)_3]^{2-}$, with the equilibrium potential of −0.737 V. In the presence of Cd ions most of the CN^- anions are consumed in Cd–CN complexes ($[Cd(CN)]^+$, $[Cd(CN)_2]$, $[Cd(CN)_3]^-$ and $[Cd(CN)_4]^{2-}$) and the dominant Ag–CN complex becomes $[Ag(CN)_2]^-$, with the equilibrium potential of −0.479 V (Table 1). Hence, from the presented analysis it is obvious that the first shoulder on a solid curve in Fig. 1 for Ag–Cd alloy deposition corresponds to the deposition of pure Ag from $[Ag(CN)_2]^-$ complex [10] which is dominant in pure Cd–CN and Ag–Cd–CN electrolytes.

Table 1
Concentration of different Ag complexes and their eqilibrium potentials.

Solution composition	Ag complexes		
	$[Ag(CN)_2]^-$	$[Ag(CN)_3]^{2-}$	$[Ag(CN)_4]^{3-}$
$-\log(K/M^{-1})$, stability constant	21.2	21.7	20.6
0.032 M $KAg(CN)_2$ 0.56 M KCN			
Concentration (mole fraction (%))	35.9	61.2	2.6
(E_{eq}/V)	−0.737	−0.737	
0.032 M $KAg(CN)_2$ 0.14 M $CdSO_4$ 0.56 M KCN			
(Concentration (%)	98.1	1.8	0.0009
(E_{eq}/V)	−0.479		

E vs. Ag/AgCl.

This is confirmed also by the composition analysis (see section 3.2).

The alloy deposition from this electrolyte is of a regular type according to Brenner's classification [1] and the cadmium content in the coatings should increase with the increase in current density (or increase of cathodic potential).

One of the conditions required for identification of the phase structure of Ag–Cd alloys by ALSV technique is the presence of sufficiently large difference between the dissolution potentials not only of pure Ag and Cd metals, but also between the dissolution potentials of the alloy phases present in the deposit [26]. To meet this requirement an appropriate electrolyte for the dissolution of the alloy coating is needed. The solution used in the present investigations contained 12 M LiCl + 0.1 M HCl. The same electrolyte was chosen and successfully applied during ALSV investigations of Ag–Pd [25] and Ag–In alloys [27]. In this case the complete dissolution, without any passivation of the silver and palladium phases and the formation of a strong Ag complex (probably $AgCl_4^{3-}$) with an instability constant of 1.2×10^{-6} were reported [25,27,31]. According to the literature data [32,33] in such high concentration of chloride ions (12.1 M) the solubility of AgCl increases up to about 0.05 M AgCl (at a given temperature) and in accordance with this statement for small amount of dissolved Ag^+ ions no precipitation of AgCl should be expected. This is clearly demonstrated in the reference [25], Fig. 3.

3.2. The ALSV and XRD analysis of Ag, Cd and Ag–Cd alloys electrodeposited at a constant potential

The ALSV curves of dissolution ($v = 1\,mV\,s^{-1}$) of pure Cd and pure Ag coatings are shown in Fig. 2. Sufficiently large difference between the dissolution potentials of the pure metals of about 0.75 V is registered. As was previously established, cadmium as the less noble constituent of the alloy is completely dissolved at more negative potentials of about −0.75 V, while the more noble silver has a dissolution peak at about 0.02 V [23–25]. Comparing the charge under the ALSV curves for Cd dissolution with the total deposition charge of $Q_{dep} = 1.3\,C\,cm^{-2}$ it was found that the current efficiency ($\eta_j = Q_{diss}/Q_{dep}$) for cadmium deposition decreases with increasing potential from about 94% (−1.0 V) to about 79% (−2.0 V), due to the increase of the contribution of hydrogen evolution reaction to the whole process of electrodeposition of cadmium at potentials more negative than −1.6 V. Similar behavior is observed for pure Ag deposition with the current efficiency of about 63% at a potential of −1.0 V and 37% at −2.0 V. In the case of Ag–Cd alloy deposition current efficiency is also found to decrease with increasing cathodic potential (from 63% at −1.0 V to 54% at −2.0 V), as in the case of deposition of pure metals.

Fig. 3 shows current transients (*j* vs. *t*), obtained during the deposition of alloys. The oscillations are not registered, possibly as a result of the co-deposition of silver, since they are not registered for deposition of pure Ag (Fig. 1, dashed line).

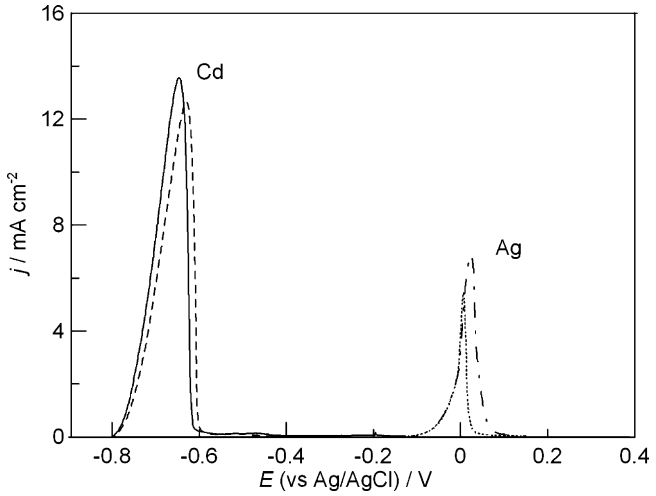

Fig. 2. ALSV curves recorded at the sweep rate of 1 mV s^{-1} for dissolution of Cd and Ag deposited at different potentials (*E*). Cd dissolution: Solid line (*E* = −1.0 V), dashed line (*E* = −2.0 V). Ag dissolution: dash-dot line (*E* = −1.0 V), dotted line (*E* = −2.0 V).

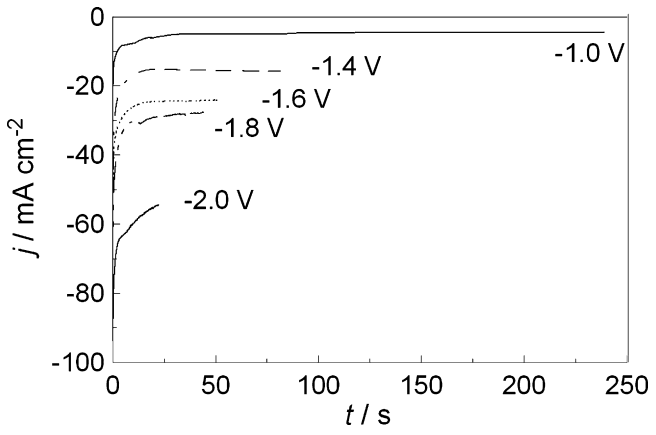

Fig. 3. Current density vs. time transients (*j*–*t*) recorded during deposition of Ag–Cd alloys to a constant charge of 1.3 C cm^{-2} at different potentials marked in the figure.

The XRD patterns, obtained just after deposition of the coatings (see Fig. 3) are presented in Fig. 4, while the ALSV curves

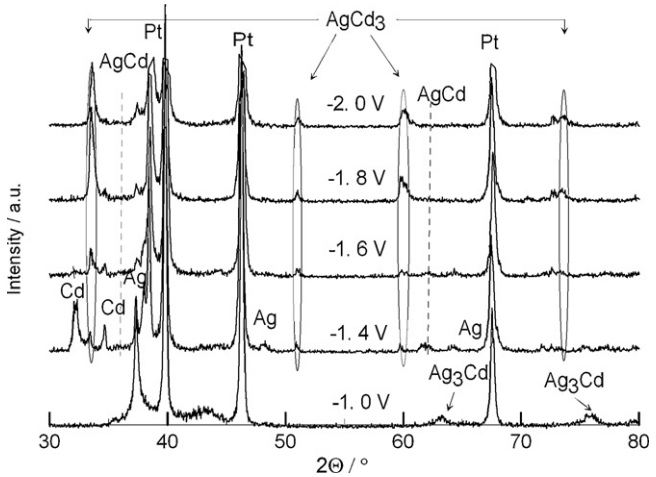

Fig. 4. XRD spectra of the alloy coatings deposited at different potentials (marked in the figure).

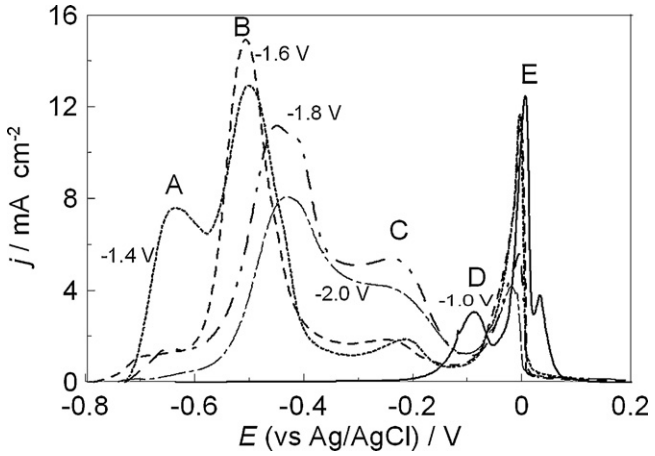

Fig. 5. ALSV curves recorded at the sweep rate of 1 mV s^{-1} for dissolution of alloys deposited under conditions presented in Fig. 3. Deposition potentials are marked in the figure.

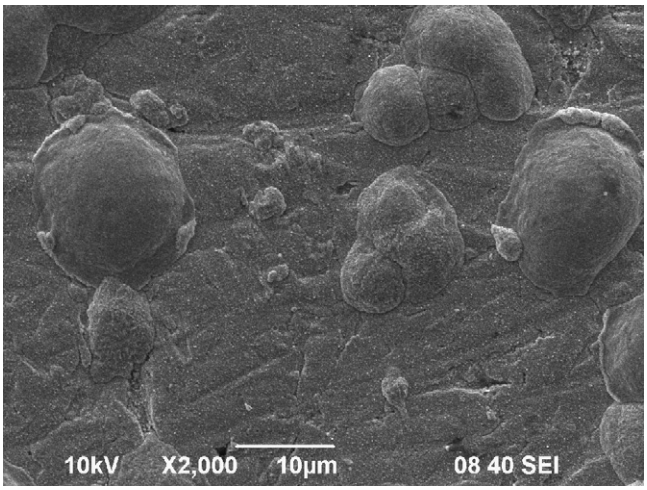

Fig. 6. Surface morphology (SEM) of the alloy coating deposited at a potential $E = -1.0$ V.

for dissolution of Ag–Cd coatings deposited at different cathodic potentials (−1.0, −1.4, −1.6, −1.8, and −2.0 V) are presented in Fig. 5.

In the coatings deposited at −1.0 V two peaks, one corresponding to pure Ag and two corresponding to the Ag_3Cd phase could be detected on the diffractogram. The Ag_3Cd phase is, according to the phase diagram [29], high-temperature phase of the Ag–Cd system which was not detected in previous investigations of electrodeposited Ag–Cd alloys [16–18,22]. A well defined peak D on the ALSV for alloy deposited at −1.0 V (Fig. 5) is the indication of the presence of Ag_3Cd phase, while the peak E corresponds to the dissolution of reprecipitated Ag [26], which is in accordance with the diffractograms shown in Fig. 4. As can be seen in Fig. 5 this peak practically disappears on the ALSVs of dissolution of alloys with higher content of Cd (ALSVs recorded for alloys deposited at −1.4, −1.6, −1.8 and −2.0 V), transforming into hardly visible shoulder, which is in agreement with the diffractograms presented in Fig. 4. Such behavior is not unexpected, since it is quite possible that its amount becomes lower with the increase of Cd content in the alloy and its detection by the X-ray technique is not possible, while on the ALSVs its presence could be hardly detected, although not as well defined peak, but as a shoulder. It is interesting that this phase is well defined on the ALSV of sample deposited at a constant current density (Fig. 9), indicating that the conditions of alloy deposition (potentiostatic or galvanostatic) produce alloys with different phases as well as with different amounts of the same phases in the deposit.

The morphology of the coating deposited at −1.0 V is presented in Fig. 6. The morphology of this coating is typical to those, described during the investigations of Jayakrishnan [22], where the gradual increase in crystalline size with increase in cadmium content is observed.

At more negative potential (−1.4 V) the coating becomes very heterogeneous (see Fig. 7a) and reflections of Cd, $AgCd_3$, AgCd and Ag phases were registered on the XRD spectra, which should correspond to the separate peaks on the ALSV curves. The heterogeneity of the coating could be the consequence of two factors: the alloy composition and the influence of simultaneous hydrogen evolution, since the natural convection must be significantly disturbed by the hydrogen evolution at this potential [8].

The ALSV curve of the alloy coating deposited at a potential of −1.4 V is characterized by the presence of three additional peaks, A, B and C (Fig. 5). The most negative peak A (at about −0.68 V) could be ascribed to the peak of pure cadmium (see Fig. 2), which is also well defined on the diffractogram presented in Fig. 4. According to some previously reported results obtained by ALSV technique the peaks in between should be attributed to different alloy phases [26]. These could be the registered $AgCd_3$ (B) and AgCd (C) phases, the latter with negligible amount according to the XRD spectra, as well as to the ALSV results.

The heterogeneity of this coating is well visible – its morphology is presented in Fig. 7a. In the rough areas of the coating the cadmium content is about 40 at.% (Fig. 7b), while in the smooth areas it reaches 58 at.% (Fig. 7c).

The deposition at higher cathodic potentials, −1.6 or −1.8 V, leads to the appearance of some periodic structured areas on the surface (Fig. 8a and b), the reflections of pure cadmium disappear (Fig. 4), which could be connected with the changes in the current efficiency and the enhanced formation of Ag–Cd alloy phases.

The corresponding ALSV curves (Fig. 5) show that the peak of pure cadmium (A) becomes smaller and practically disappears in the alloys deposited at the most negative potential (−2.0 V), while the next one (B), corresponding to the dissolution of cadmium-rich phase, grows. It could be seen that the peak of $AgCd_3$ phase dissolution (B) appears at more positive potentials for alloys deposited at −1.8 V and −2.0 V, indicating that its amount in the deposit increases. There is a certain difference between the X-ray and ALSV analysis for these two alloys. According to the ALSV results the amount of the AgCd phase increases (peak C becomes more pronounced, Fig. 5), while this phase disappears on the diffractograms (Fig. 4). Such a behavior could be the consequence of high intensity of $AgCd_3$ peaks on the diffractograms, masking the peaks corresponding to the AgCd phase.

At the most negative potential of −2.0 V preferentially the phase $AgCd_3$ is formed and mainly the corresponding reflections of this phase are registered on the XRD spectra. This is in agreement with the ALSV results, where the peak of $AgCd_3$ phase dominates over all other peaks.

The morphology of a coating deposited at a potential of −2.0 V is shown in Fig. 8c. The surface is smooth and shiny, indicating the presence of mainly one phase in the deposit ($AgCd_3$).

Comparing the results of XRD and ALSV phase analysis of alloys deposited at a constant potentials it could be stated that satisfactory agreement has been obtained.

3.3. The ALSV and XRD analysis of Ag–Cd alloys electrodeposited at a constant current density

The deposition under galvanostatic conditions, which is used in the practice, offers the possibility for a stronger heterogeneity

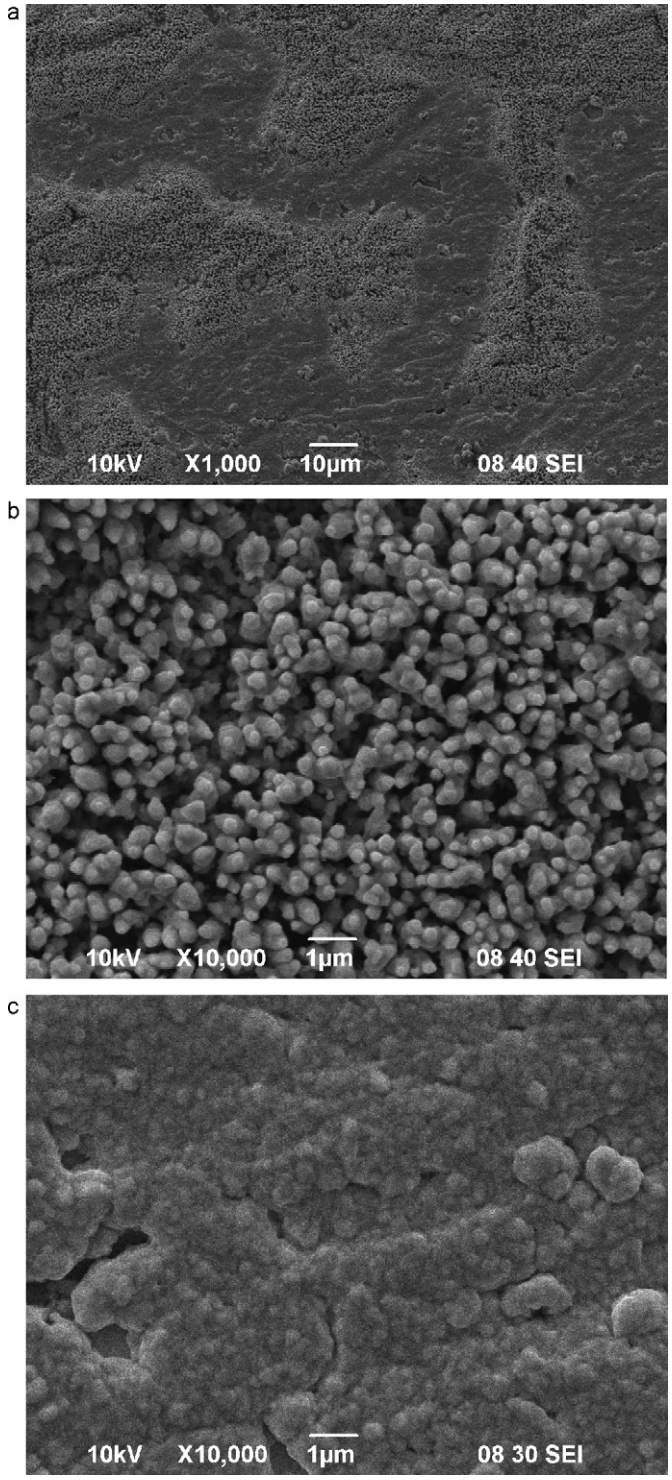

Fig. 7. (a) Surface morphology (SEM) of the alloy coating deposited at $E = -1.4$ V. (b) and (c) different areas of the same coating at higher magnification.

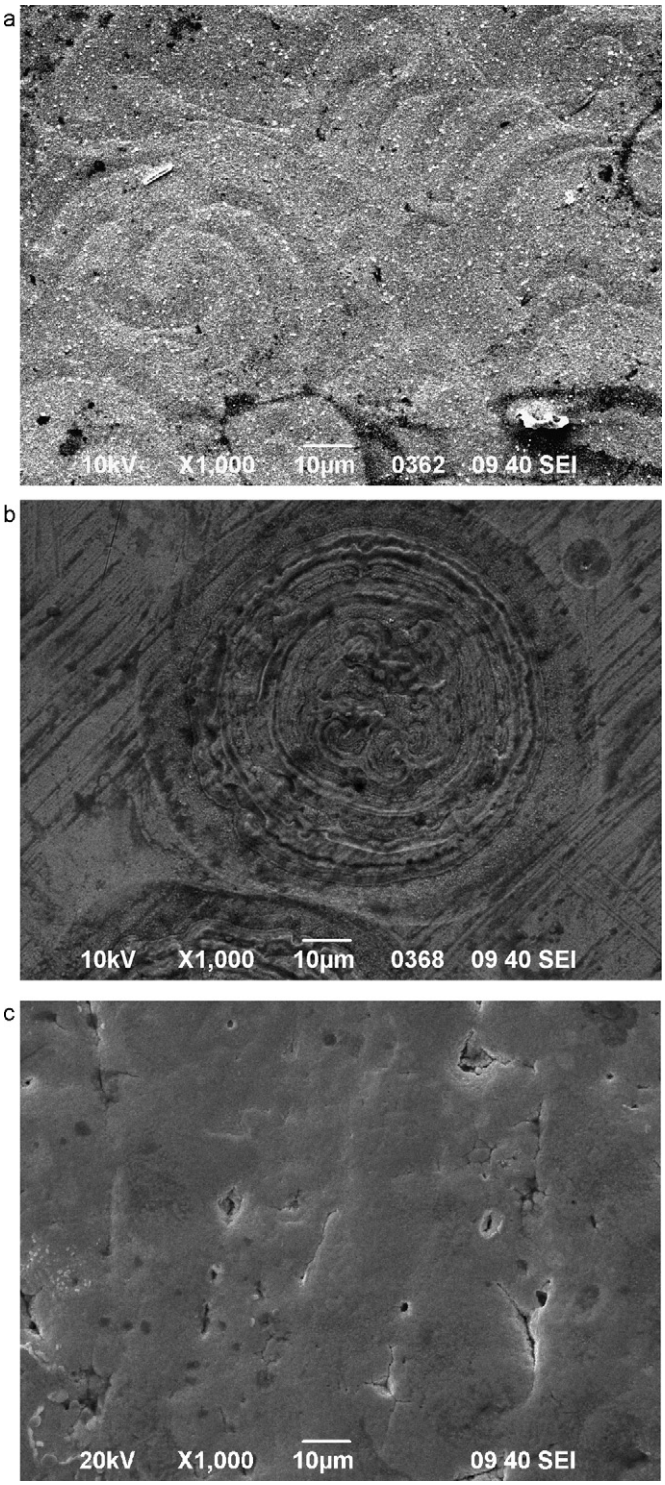

Fig. 8. Surface morphology (SEM) of alloy coatings deposited at different (more negative) potentials: (a) $E = -1.6$ V; (b) $E = -1.8$ V; (c) $E = -2.0$ V.

of the coatings and possibly for better differentiation of the separate phases of the alloy. The observed heterogeneity is impressive due to the formed spatio-temporal structures [10]. In Fig. 9 are presented ALSV of Ag–Cd alloy dissolution deposited at a constant current density of $-2.5\ \mathrm{mA\,cm^{-2}}$ and corresponding E–t response for deposition (in the inset). The oscillations of the potential (Fig. 9 inset) are most probably due to the formation of spatio-temporal structures, which are also connected with the hydrogen evolution reaction [10,30]. The oscillations of potential or current density during the Ag–Cd alloy deposition will be the subject of our future investigations.

As can be seen all peaks corresponding to dissolution of certain phases (A, B, C, D and E) are much better defined in comparison with those for alloys deposited at a constant potential, indicating that during galvanostatic deposition better separation of the ALSV peaks could be obtained, most probably as a consequence of more pronounced heterogeneity of the alloy.

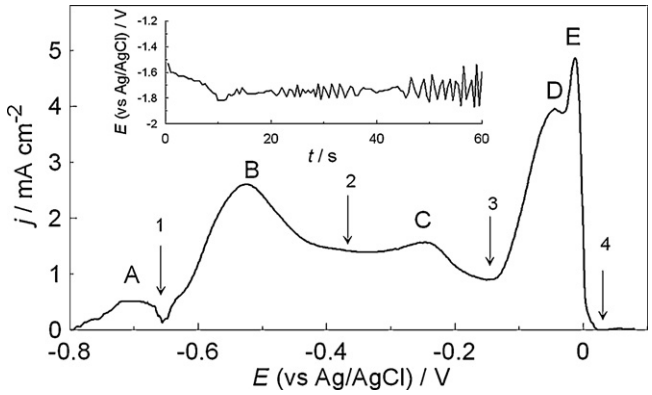

Fig. 9. ALSV curve recorded at the sweep rate of $1\,mV\,s^{-1}$ of the alloy coating deposited at a constant current density $j = -2.5\,mA\,cm^{-2}$. Corresponding E–t response for alloy deposition is shown in the inset.

In order to find the exact correlation between the ALSV peaks and the phases in the coating deposited under galvanostatic conditions ($2.5\,mA\,cm^{-2}$) in the first step only the phase corresponding to the first peak A was dissolved (arrow 1 in Fig. 9). In the separate runs the potential was swept to the arrows 2–4 marked in the figure. During the second sweep, starting from the same potential (−0.80 V), the phases corresponding to the first (A) and to the second (B) peaks were dissolved; in the third sweep – the phases corresponding to the A, B and C peaks were dissolved, while practically whole deposit was dissolved at the potential marked with the arrow 4.

The parallel XRD investigations of the as-deposited layer and of the layer after electrochemical treatments (ALSV) are depicted in Fig. 10. Fig. 11 shows cut-outs of the patterns in the 2θ range between 36° and 41°.

In the as-deposited layer the following reflections were identified: all reflections of the hexagonal $Ag_{1.05}Cd_{3.95}$ phase with very high intensity of the (0 0 2) orientation, the (1 0 0) reflex of hexagonal Cd, the (1 1 0) reflex of cubic AgCd and all reflections of the Pt substrate (Figs. 10 and 11). Therefore the main phase is the $Ag_{1.05}Cd_{3.95}$ phase. This phase shows a preferred ⟨0 0 1⟩ orientation. The fractions of ⟨1 1 0⟩ orientated AgCd and ⟨1 0 0⟩ orientated Cd are much smaller. It should be stated here that Ag_3Cd phase, well defined on the ALSV (peak D) has not been detected by the

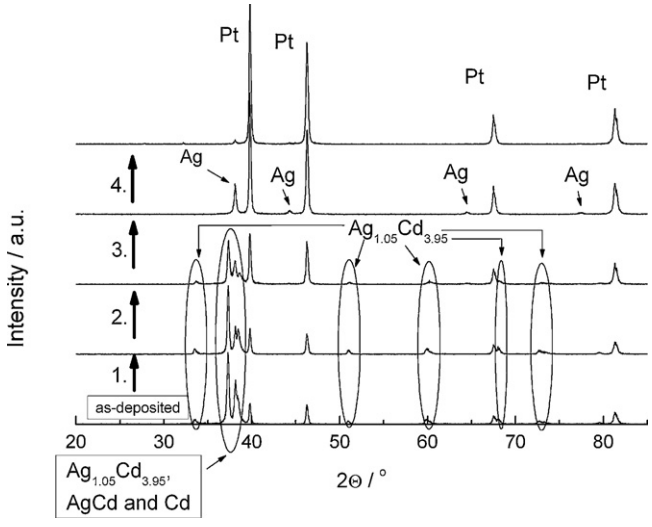

Fig. 10. XRD spectra at different stages of dissolution of the coating deposited at a constant current density (Fig. 9).

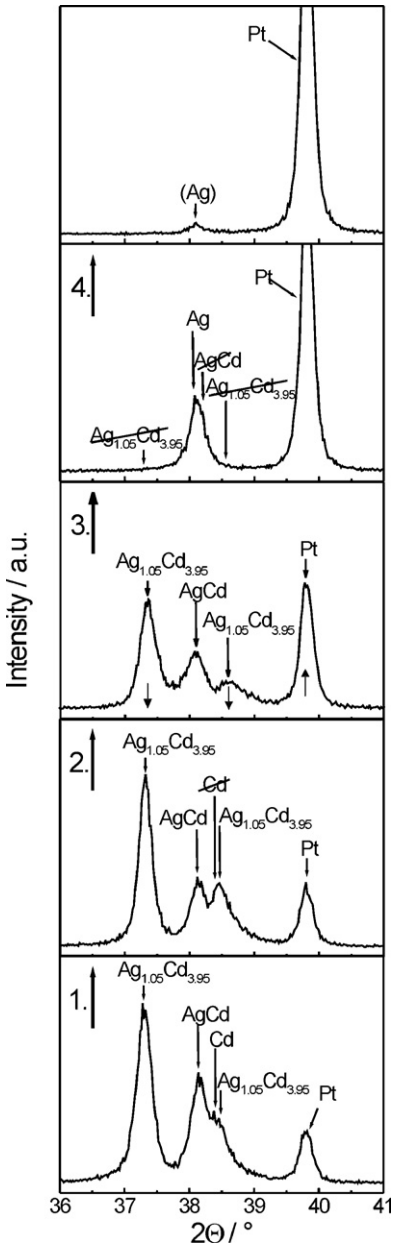

Fig. 11. Cut-outs (between $2\theta = 36°$ and $2\theta = 41°$) of the X-ray patterns presented in Fig. 10.

X-ray technique. At the present stage of investigations the authors cannot offer reasonable explanation for such behavior, but this phenomenon will be the subject of our more detailed investigations of the system Ag–Cd.

After dissolving the phase corresponding to peak A by the ALSV a new XRD spectrum is recorded. In the second diffractogram the peak of pure Cd disappears (Fig. 11, curve 2), but the other phases $Ag_{1.05}Cd_{3.95}$ and AgCd are still registered. Instead of $AgCd_3$ phase (PDF 028-0199), detected in samples deposited at a constant potential, phase $Ag_{1.05}Cd_{3.95}$ (PDF 065-7991) has been detected in the sample deposited at a constant current density (they have the same space group $P63/mmc$).

After the next dissolution step, in the potential range between −0.8 and −0.3 V (arrow 2 in Fig. 9) the phase corresponding to the potential of the next peak B, was not totally dissolved. About the half of the intensity of the $Ag_{1.05}Cd_{3.95}$ reflections remained, thus, about the half of this phase has been dissolved in this step.

After the next dissolution step in the potential range between −0.8 and −0.1 V (arrow 3 in Fig. 9) the XRD measurement shows the absence of any Cd containing phases, only the characteristic peaks of Ag and Pt are registered (Figs. 10 and 11, curve 4). Accordingly, the whole amount of cadmium is dissolved and only silver remained in the deposit. In the last step this silver is dissolved (nearly completely) and only the peak of the platinum substrate has been detected.

Considering the ALSV curves shown in Figs. 5 and 9 and the results of the X-ray analysis presented in Figs. 4, 10 and 11 following statements could be made:

- the peak A corresponds to the pure Cd-phase;
- the peak B corresponds to the $Ag_{1.05}Cd_{3.95}$ phase in sample deposited at a constant current density;
- the same peak corresponds to the $AgCd_3$ phase in samples deposited at a constant potential;
- the peak C corresponds to the AgCd phase;
- the peak D corresponds to the Ag_3Cd phase in samples deposited at a constant potential;
- the peak E corresponds to the pure Ag.

Considering the phase diagram of the alloy system Ag–Cd [28] it appears that each phase exists in a very broad atomic percentage range. The potential interval of each phase registered by ALSV technique depends on the percentage range of its existence. Taking into account that the distribution of Cd in the coating is non-homogeneous, one can expect the change of the position of some peaks on the ALSV.

4. Conclusions

Different phases (Ag, Ag_3Cd, AgCd, $AgCd_3$ and pure Cd) are observed in the coatings deposited at different cathodic potentials. A good correlation between the XRD spectra of the Ag–Cd alloy coatings and the ALSV data obtained during their dissolution is established.

In the case of Ag–Cd alloy deposited at a constant current density instead of the $AgCd_3$ phase, $Ag_{1.05}Cd_{3.95}$ phase has been detected by the X-ray analysis at the position of the ALSV peak B, while the Ag_3Cd phase, characterized by well defined peak D on the ALSV, was not detected on the corresponding diffractogam.

Acknowledgements

The authors express their gratitude to Deutsche Forschungsgemeinschaft (DFG) (Project 436 BUL 113/97/0-4), as well as to the Ministry of Science and Technological Development of the Republic of Serbia, for financial support of this work.

References

[1] A. Brenner, Electrodeposition of Alloys. Principles and Practice, vol. 2, Academic Press, New York, London, 1963, p. 658.
[2] K.M. Gorbunova, Yu. Polukarov, Electroosazhdenie metallov i splavov, Itogi nauki, Moskva, 1966, p. 59.
[3] E. Raub, A. Schall, Z. Metallkd 30 (1938) 149.
[4] I. Kristev, M. Nikolova, J. Appl. Electrochem. 16 (1986) 875.
[5] I. Krastev, M.T.M. Koper, Physica A 213 (1995) 199.
[6] I. Krastev, T. Valkova, A. Zielonka, J. Appl. Electrochem. 33 (2003) 1199.
[7] A. Hrussanova, I. Krastev, J. Appl. Electrochem. 39 (2009) 989.
[8] Ts. Dobrovolska, L. Veleva, I. Krastev, A. Zielonka, J. Electrochem. Soc. 152 (2005) C137.
[9] Ts. Dobrovolska, I. Krastev, A. Zielonka, Russ. J. Electrochem. 44 (2008) 676.
[10] Ts. Dobrovolska, I. Krastev, A. Zielonka, ECS Trans. 25 (2010) 1.
[11] I.R. Epstein, Physica D 51 (1991) 152.
[12] A.M. Turing, Philos. Trans. R. Soc. London, Ser. B 237 (1952) 37.
[13] I. Prigogine, Science 201 (1978) 777.
[14] M.C. Cross, P.C. Hohenberg, Rev. Mod. Phys. 65 (1993) 851.
[15] A.S. Mikhailov, G. Ertl, Chem. Phys. Chem. 10 (2009) 86.
[16] C.W. Stillwell, J. Am. Chem. Soc. 53 (1931) 2416.
[17] C.W. Stillwell, L.E. Stout, J. Am. Chem. Soc. 54 (1932) 2583.
[18] C.W. Stillwell, H.I. Feinberg, J. Am. Chem. Soc. 55 (1933) 1864.
[19] I. Nambissan, A.J. Allmand, Trans. Faraday Soc. 47 (1951) 303.
[20] L.N. Rastorguev, I.D. Kudryavtseva, E.A. Kislitsyn, S.A. Barinov, V.M. Momotova, Sov. Electrochem. 11 (1975) 1696.
[21] L.W. Flott, Met. Finish. 83 (1985) 11.
[22] S. Jayakrishnan, Trans. Inst. Met. Finish. 78 (2000) 124.
[23] V.D. Jovic, R.M. Zejnilovic, A.R. Despic, J.S. Stevanovic, J. Appl. Electrochem. 18 (1988) 511.
[24] V.D. Jovic, S. Spaic, A.R. Despic, S. Stevanovic, M. Pristavec, Mater. Sci. Technol. 7 (1991) 1021.
[25] V.D. Jovic, B.M. Jovic, A.R. Despic, J. Electroanal. Chem. 357 (1993) 357.
[26] A.R. Despic, V.D. Jovic, in: R.E. White, J.O.M. Bockris, B.E. Conway (Eds.), Modern Aspects of Electrochemistry, vol.27, Plenum Press, 1995, p. 143.
[27] Ts. Dobrovolska, V.D. Jovic, B.M. Jovic, I. Krastev, J. Electroanal. Chem. 611 (2007) 232.
[28] M. Hansen, K. Anderko, Constitution of Binary Alloys, McGraw-Hill, New York, 1958, p.26.
[29] Landolt-Bornstein, Database Numerical Data and Functional Relationships in Science and Technology, Springer, 1991, p. 1, IV-5A.
[30] N. Kaneko, H. Nezu, N. Shinohara, J. Electroanal. Chem. 252 (1988) 371.
[31] Spravochnik Himika, second ed., Himia, Moskva, 1965, pp. 119-167.(Russ.).
[32] U. Cohen, K.R. Walton, R. Sard, J. Electrochem. Soc. 131 (1984) 2489.
[33] U. Cohen, F.B. Koch, R. Sard, J. Electrochem. Soc. 130 (1983) 1987.